

## Extended X-ray absorption fine structure (EXAFS) investigations of Ti bonding environment in sputter-deposited nanocomposite TiBC/a-C thin films

This content has been downloaded from IOPscience. Please scroll down to see the full text.

2010 IOP Conf. Ser.: Mater. Sci. Eng. 12 012012

(<http://iopscience.iop.org/1757-899X/12/1/012012>)

View [the table of contents for this issue](#), or go to the [journal homepage](#) for more

### Download details:

IP Address: 161.111.154.24

This content was downloaded on 18/11/2014 at 07:32

Please note that [terms and conditions apply](#).

# Extended X-ray absorption fine structure (EXAFS) investigations of Ti bonding environment in sputter-deposited nanocomposite TiBC/a-C thin films

J L Endrino<sup>1</sup>, M D Abad<sup>2</sup>, R Gago<sup>1</sup>, D Horwat<sup>3</sup>, I Jiménez<sup>1</sup> and J C Sánchez-López<sup>2</sup>

<sup>1</sup> Instituto de Ciencias de Materiales de Madrid, Consejo Superior de Investigaciones Científicas, Campus de Cantoblanco, E-28049 Madrid, Spain

<sup>2</sup> Instituto de Ciencia de Materiales de Sevilla, CSIC-Universidad de Sevilla, Avda. Américo Vespucio 49, 41092 Sevilla, Spain

<sup>3</sup> Institut Jean Lamour, Département CP2S, Nancy Université, Ecole des Mines, CS14234 Parc de Saurupt, 54042 Nancy Cedex France

E-mail: jlendrino@icmm.csic.es

**Abstract.** In this study, we have successfully used the extended X-ray absorption fine structure (EXAFS) technique at the Ti-K edge to extract the local structure in a set of nanocomposite TiBC/a-C coatings deposited by a combined d.c.-pulsed and r.f.-magnetron sputtering deposition process. The sequence of Fourier transform spectra in the deposited films shows that there is an increase in the number of Ti-C bonds in the films of higher carbon content in parallel with the increment of the total carbon content. In addition, Ti-K EXAFS spectra indicate that in all the deposited TiBC/a-C films, first-shell neighbours are in a nearer structural arrangement than the one expected for a bulk hexagonal TiB<sub>2</sub>, which could be due to the formation of mixed Ti-B-C compound in a structural unit similar to the one found in h-TiB<sub>2</sub>.

## 1. Introduction

TiBC/a-C nanocomposites are promising materials as protective coatings for machine and tool elements due to the appropriate combination of crystalline hard phases (borides, carbides) and amorphous carbon as phase boundary. This nanoscaled heterostructure allows combining hardness with other interesting properties for engineering applications as low friction coefficient, wear resistance and toughness. In particular, the presence of carbon and boron may be suitable to further improve the tribological performance by forming self-lubricious compounds that can work both at room and at high temperature. Clearly, it is of a key technological importance to resolve the phases formed and bonding environment in TiBC/a-C nanocomposites. However, traditional diffraction techniques cannot be effectively employed to extract complete structural information in complex nanostructured films due to the absence of long-range order.

## 2. Experimental

### 2.1 Sample preparation

The TiBC/a-C nanocomposite coatings were prepared by Ar<sup>+</sup> sputtering of a combined TiC:TiB<sub>2</sub> (60:40) and graphite targets. The magnetron sources were r.f. (graphite target, Goodfellow, 99.5%) and pulsed d.c. (TiC:TiB<sub>2</sub> target) at frequencies of 13.56 MHz and 50 kHz respectively. The pressure of the vacuum chamber was measured before deposition in 3×10<sup>-4</sup> Pa and 0.60 Pa during film growth. A series of TiBC/a-C coatings has been prepared by changing the sputtering power ratio (R), defined as the ratio of sputtering power applied to the graphite target in respect to the TiC:TiB<sub>2</sub> one (R= P<sub>C</sub>/P<sub>TiC:TiB<sub>2</sub></sub>), from 0 to 3. The typical power values applied to the TiC:TiB<sub>2</sub> and graphite targets are summarized in Table 1. A rotation speed of 10 rpm is used to ensure homogeneity. The temperature was found to vary in the range of 150–200 °C under the effect of the plasma. No additional heating of the substrate was done. A negative d.c. bias of 100V was applied to the samples during whole deposition process. The growth time was around 5 hours and the film thickness ranges from 1.0 to 1.5 μm. The substrates used were silicon and M2 steel. More details concerning the deposition process can be found elsewhere [1].

### 2.2 Sample characterization

The crystal structure of the films was examined by X-ray diffraction analysis (XRD) at 1° of incidence angle using Cu Kα radiation in a Siemens D5000 diffractometer. A Philips CM200 microscope operating at 200 kV and equipped with a parallel detection electron energy-loss spectrometer (EELS) from Gatan (766-2k) was used for evaluation of the film chemical composition. The estimated atomic percentages for the coatings are shown in Table 1 as a function of the synthesis conditions. X-ray absorption near edge structure (XANES) and extended X-ray absorption fine structure (EXAFS) measurements at the Ti-K edge were conducted at the KMC2 beamline at the electron storage ring BESSY in Berlin. The beamline is equipped with a double crystal SiGe(111) monochromator. The measurements were carried out in total fluorescence yield mode (TFY). The collected EXAFS data was analyzed using Athena analysis software (version 0.8.056). E<sub>0</sub> was chosen to be 4965eV and the spectra were normalized between 150eV and 500eV above the edge. The k-range used for the R-space data analysis of all the samples was from 3.8 to 9.0, no coordination number data is reported here due to space limitations.

**Table 1.** Synthesis conditions and chemical composition of TiBC/a-C samples measured using EELS.

|           | P <sub>TiC:TiB<sub>2</sub></sub><br>(W) | P <sub>C</sub><br>(W) | Ti<br>(at.%) | B<br>(at.%) | C<br>(at.%) | TiB <sub>x</sub> C <sub>y</sub> stoichiometry |
|-----------|---|-----------------------|--------------|-------------|-------------|---|
| <b>R0</b> | 250                                     | 0                     | 45.0         | 23.8        | 31.2        | TiB <sub>0.53</sub> C <sub>0.70</sub>         |
| <b>R1</b> | 250                                     | 250                   | 38.8         | 12.0        | 49.2        | TiB <sub>0.31</sub> C <sub>1.27</sub>         |
| <b>R2</b> | 125                                     | 250                   | 24.6         | 14.4        | 61.0        | TiB <sub>0.59</sub> C <sub>2.48</sub>         |
| <b>R3</b> | 125                                     | 375                   | 16.4         | 12.3        | 71.3        | TiB <sub>0.75</sub> C <sub>4.35</sub>         |

## 3. Results and discussion

### 3.1 X-ray diffraction and X-ray absorption near edge structure

XRD spectra in figure 1 show a slight increase in the intensity of two broad peaks (at around 20~34° and 59°) with the increment in carbon content within the film. However due to the proximity of the diffraction peaks for face centered cubic (fcc-TiC) and hexagonal (h-TiB<sub>2</sub>) phases together with the marked nanocrystalline or quasi-amorphous nature it is not possible to discriminate them. In addition, this peak can be also attributed to a ternary phase including Ti, C and B [1]. X-ray absorption near edge spectra (figure 2) of TiBC/a-C films in the near Ti-K edge region show fine structures in between h-TiB<sub>2</sub> and fcc-TiC. The slight changes in the lineshape of the deposited TiBC/a-C films and certain energy shift of the edge (~1 eV) are consistent with an increase in the content of cubic domains with the carbon addition in the samples.

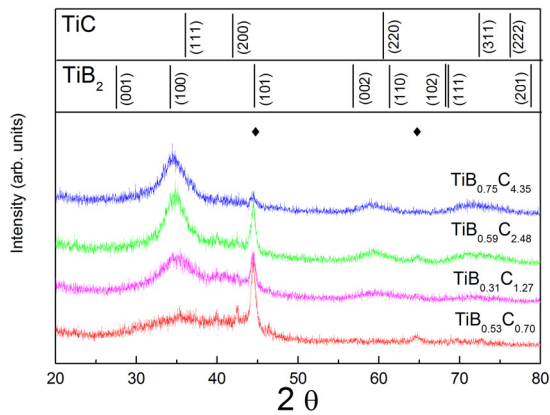


**Figure 1.** XRD patterns for the four TiBC/a-C deposited samples. (◆) corresponds to the steel substrate.

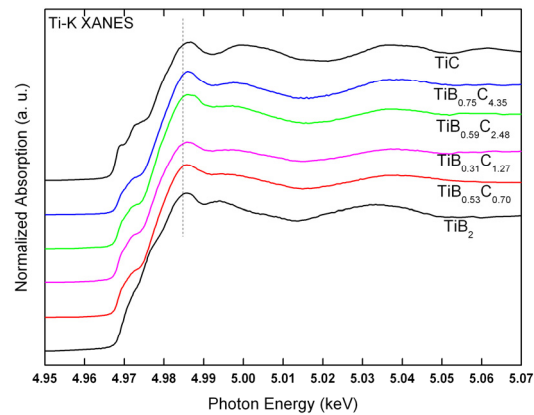


**Figure 2.** Normalized X-ray absorption near-edge structure (XANES) data for TiBC/a-C samples together with those of fcc-TiC and h-TiB<sub>2</sub> standards.

### 3.2 Extended X-ray absorption fine structure

EXAFS spectrum measured above the absorption edge of titanium atoms provides information on the local structure independently of the amorphous or crystalline nature of the phases probed. The  $k^2$  weighted EXAFS signals as a function of  $k$  are shown in figure 3. The spectra show that the sample with lowest carbon has the lowest amplitude of oscillations of the set. The samples with higher carbon show an increase in amplitude of the oscillations corresponding to the cubic character.

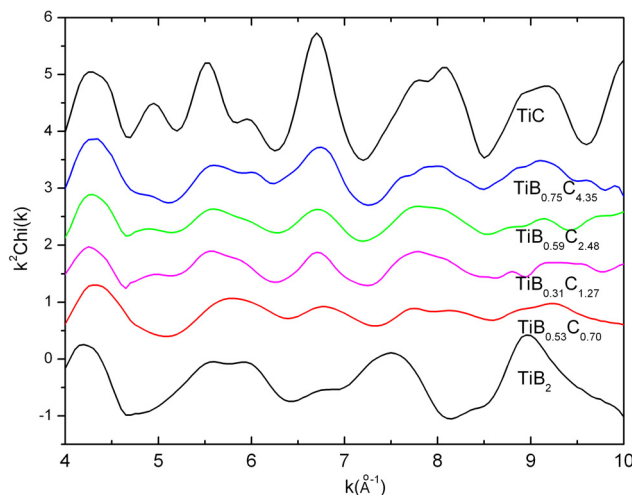


**Figure 3.**  $k^2$ -weighted EXAFS,  $k^2\chi(k)$ , of TiBC/a-C samples as a function of the photoelectron wave number  $k$ , together with fcc-TiC and h-TiB<sub>2</sub> standards.

Basic structural information around the titanium atoms can be extracted directly from the Fourier transformations (FT) of the EXAFS signals even before detailed quantitative analysis, which is not shown here due to space limitations. Unlike in the XANES spectral data, the FT-EXAFS signals of the fcc-TiC and h-TiB<sub>2</sub> differ so much that only the nearest neighbor information (up to 4 Å) of the TiBC/a-C films is enough to have an insight of the phases present in the samples. Figure 4 depicts the sequence of FT spectra for the nanocomposite films with two main peaks at (~1.3-1.6 Å) and ~2.4 Å. While the second peak has a close correspondence with the main peak measured for fcc-TiC standard and reported for a-TiC films [2], the first peak does not correspond exactly with first shell peak in the h-TiB<sub>2</sub> standard (at ~1.8Å) or reported in amorphous/nanocrystalline TiB<sub>2</sub> phase at 1.7Å [3]. This

EXAFS R-position shift could be associated to the presence of Ti-B bonds in a ternary  $\text{TiB}_x\text{C}_y$  phase originated by distortion of a hexagonal  $\text{TiB}_2$  phase by introducing C atoms [1]. Clearly, this shift is slightly different, than the alpha ( $\Delta r$ ) shift reported for  $\text{TiB}_2$  [3] and could be in part due to a change in composition in the hexagonal domains. In contrast, the location of the second peak (attributed to Ti-C bonds) remains unaffected in most of the samples. The increase of the relative intensity of the second peak manifests an increased Ti-C bonding character as the carbon content increases either in nanocrystalline TiC and/or  $\text{TiB}_x\text{C}_y$  phases.

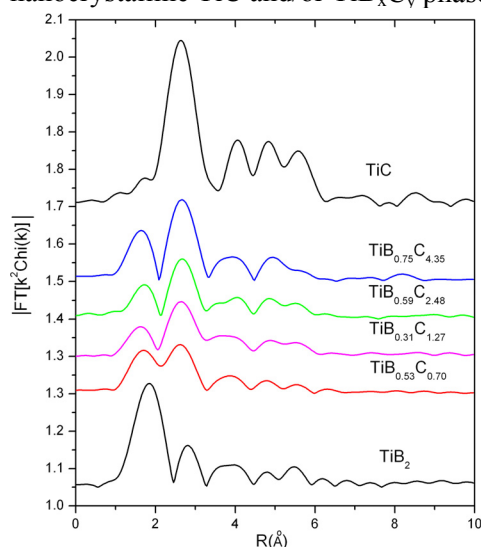


**Figure 4.** Magnitude of the non-phase corrected Fourier transform of  $k^2\chi(k)$  to position space,  $|\chi'(R)|$ , of TiBC/a-C samples as a function of distance  $R$  (Å), together with those of fcc-TiC and h-TiB<sub>2</sub> standards.

#### 4. Conclusions

First exploratory X-ray absorption experiments at the Ti-K edge have been carried out in a set of TiBC/a-C films with various boron and carbon contents. While X-ray diffraction and XANES yielded only limited information about these compounds, preliminary EXAFS observations at the Ti-K edge indicate that EXAFS is a suitable technique to study the atomic arrangement in TiBC/a-C nanocomposite films. Firstly it was observed that there was a shift between the position of nearest FT-EXAFS peak in the samples and the one observed and reported for the  $\text{TiB}_2$  phase. This shift could be due to the formation of a ternary  $\text{TiB}_x\text{C}_y$  phase. In addition, the second nearest peak in the FT-EXAFS signal of nanocomposite TiBC/a-C was identified to correspond to Ti-C bonds, given the good agreement between the position of this peak and the predominant peak of fcc-TiC, and also reported for a-TiC films. The gradual increase in the intensity of this peak with carbon addition agrees with a gradual transformation from a hexagonal arrangement around Ti atoms towards another containing more cubic domains

#### Acknowledgements

This work was partially supported by the Spanish Ministry of Science and Education through projects Consolider CSD2008-00023, MAT2007-66881-C02-01 and European Union (NOE EXCELL NMP3-CT-2005-515703). Travel and accommodation to BESSY II was granted by “Integrating Activity on Synchrotron and Free Electron Laser Science (IA-SFS)” EU program.

#### References

- [1] Abad M D, Cáceres D, Pogozhev Y S, Shtansky D V, Sánchez-López J C, 2009 Plasma Process Polym. **6** S107-S112
- [2] Kaloyeros A E, Williams W S, Brown F. C., Greene A E and Woodhouse J. B., 1988 Phys. Rev. B **37** 771-774
- [3] Kaloyeros A E, Hoffmann M P, Williams W S, Greene A E and McMillan J A, 1988 Phys. Rev. B **38** 7333-7344